

Multistatic Passive Radar for drone detection based Random Finite State

Milembolo Miantezila Junior^{1*}, Guo Bin², Wu Jinshuang³, Ma Weijiao³

¹Changchun University of Science and Technology, Changchun, Jilin, China.

²Zhongshan Institute of Changchun University of Science and Technology, Zhongshan, Guangdong, China.

³Intelligent Embedding Technology and Affective Computing Laboratory, Zhongshan, Guangdong, China.

Corresponding Author: 2018300111@mails.cust.edu.cn (MMJ).

Received August 31, 2023; Revised October 23, 2023; Accepted January 15, 2024

Abstract

Considering the implication of radar sensors in our daily life and environment. Localizing and identifying drones are becoming a research with a greater focus in recent years. Consequently, when an unmanned aerial vehicle is used with bad intention, this can lead to a serious public safety and privacy problem. This study investigate practical use of spectrum range for multistatic passive radar (MSPR) signal processing. Firstly, signal processing is performed after MSPR sensing detection range, this include multipath energy detection, reference signal extraction, and receiving antenna configuration. Secondly, based on the MSPR nature, the reference signal is extracted and analyzed. In addition, taking into consideration the vulnerability of passive radar when comes to a moving target localization and real time tracking detection, a novel method for spectrum sensing and detection which relies on Gaussian filter is proposed. The main goal is to optimize the use of the reference signal extracted with minimum interference as the shared reference signal in spectrum sensing. This will improve the system detection capability and spectrum access. Finally, a recursive method based on Bernoulli random filter is proposed, this takes consideration of drone's present and unknown states based on time. Moreover, a system is developed meticulously to track and enhance detection of the target. A careful result of the experiment demonstrated that spectral detection can be achieved accurately even when the drone is moving while chasing its position. It shows that Cramer Rao lower error bounds remains significantly within 3% range.

Keywords: Massive MIMO, Passive Radar, UAV, Detection, Spectrum Sensing.

1. Introduction

To give insights into practical use of single-antenna digital television-based passive radar (SDPR) detection sensing in the sense of signal processing

has been considered, and this involves multipath sensing, reference signal extraction, and antenna configuration. Reference signal extraction has been studied according to the nature of the passive radar. Knowing that it's difficult for a normal antenna digital television based passive radar (SDPR) to track and localize the targets, a unique smooth distribution has been implemented, where we take advantage of Bernoulli random finite state (BRFS). Here we put more attention on drone's emission states, its next move is treated as a hidden state, therefore a recursive random process was analyzed based on reference signal. The approach led to a systematic extraction of the reference signal, where optimal interference cancellation is performed from the receiver at the common channel, this can resist heavy interference, and optimize detection system considerably. Furthermore, the strength of the methods dwells on a deep and thoughtful experiment. However, it has been demonstrated that an UAV can become very harmful if used intentionally for a wrong motive, specially when other sensing method is added to it for data extraction and analysis [1].

2. RELATED WORKS

A study based on drone's destruction was released here [2],[3], the main approach was to create a cooperative radar sensing system for rogue drone tracking. The authors presented rogue drones in form of a stochastic dynamic process and its trajectory was systematically analyzed over time. The authors also highlighted that the moving agents presented a limited sensing rate. And the UAV can be detected with an error probability of about 1%. Consequently, there has been a number of studies in recent years focusing on detection sensing of the target and radar micro-Doppler [4],[5],[6],[7],[8],[9],[10],[11].

A study that relied on Time Velocity Diagrams (TVDs) for airborne single and multitarget moving objects [12],[13],[14], reveals a simulation experimental result for X-band sensors. They focused on studying the characteristics of one and more antennas, a number of clusters, this includes an integration of short and longer periods of time. The fact is that the system performs well, but the simulation time processing is too slow, and this can affect the test performance. Moreover, the system didn't prepare room for additional parameters like the change of weather. A spectrum sharing based Doppler frequency has been proposed in [15], here spectrum access was studied without time resolution. Doppler frequencies were used by boosting the classifier. Simulation results showed that a sensing detection was able to track the airborne moving target through the radar signal, and some detection performance were known. A good application technique based on wideband antenna such as ultra-wideband (UWB) to be used for target detection is presented [16, 17], here the receiver's antennas were used to increase the gain at about 2.4 GHz for radar and a single antenna receiver of about 800 MHz were studied. [18] described an Inertial Navigation System sensor for Pedestrian Dead Stop (PDR). They presented Kalman filter algorithm and zero-velocity sensing method for a single UWB. Spheric

polarization method which frequency band was between 1.5Ghz and 1.65Ghz was presented here [19], and an antenna array struction mapping is suggest [20], with a Rogers Duroid 5880LZ material size 29mm X 39mm was used.

A single antenna detection system for drone is presented here [21], where the strongest signal reference channel were elaborated [22],[23],[24],[25],[26] . They have presented the importance and use of received signal strength for an UAV detection.

3. ORIGINALITY

In this work, we tried to address the problem of spectrum access for multistatic passive radar signal processing based Bernoulli random finite states for drone detection. Here, unmanned aerial vehicles (UAV) and multistatic passive radar systems share interference on the same band. Our most important objectif is to extract the reference signal , analyse it, and track the target signal to understand movement , localization and intention. To bring more insight into multistatic passive radar ,our contributions can be summarized as follows:

- 1) Range detection analysis for signal processing, this includes multipath fading energy measurement , extraction of the reference signal, and configuration of the receiving antenna. Drone's tracking localization estimation of the unknown emission states is analized and we proposed a new sensing technique for UAV movement estimation. In this new approach, tracking of the target can't be disturbed including its emission state. Thus, the approach came to overcome the initial technique which doesn't consider the dynamic emission of a moving UAV. We take advantage of the referential signal extracted from the receiver with less interference as a common reference signal in multistatic passive radar,and this can be resistant to interference.
- 2) We also presented a new computation for multistatic passive radar and UAV spectrum access, this relied on the dynamic Bayesian filter method. Our particularity is that we estimate UAV's unknown emission state as a Markov hidden state. Considering the restraint data available for cognitive radio-based spectrum access, the received signal strength was used recursively to calculate the two hidden random process states of the emitter. Meanwhile, the approach is a potential extension for other applications such as spectrum access between MIMO radar, 6G mobile communication, and signal processing.
- 3) Lastly, a multi-target hidden state estimation method has been developed. This is based on Bernoulli random finite state (BRFS).Its emission states including associated hidden states are analyzed for multi-target optimal detection. Bayesian inference was used to calculate recursively UAV's present and future states by generating a dynamic stochastic process. This often is difficult e to obtain in real live. By strengthening the tracking process, the prior inference is adjusted accordingly. This was backed up by an extensive numerical experience .Thus, the system is not only

effective but also in the process of signal reference extraction, estimation, location, and detection, including uncertainty of reception, they all can be measured, therefore, the spectrum sensing can constantly be improved.

The rest of the paper is organized as follows: the sensing methodology, dynamical states, dynamical positioning, statistical detection of the drone and signal processing are presented in Section 4. In Section 5, we present the numerical experiment and performance analyses. We discussed the performance in detail and presented some applications. Section 6 is the conclusion of the paper.

4. SYSTEM DESIGN

The signal processing flow for a multistatic passive radar processing (MSPR) based Bernoulli Random Finite State (BRFS) presented here Figure 1. Firstly, after synchronization, we extracted the reference signal from the receiver's clock channel. Next, multipath clutter and direct path are performed via reference signal sample extraction. Thirdly, Matched filter-based Bernoulli random finite state (BRFS) between the performance of suppressed signal monitoring and the extracted reference. Lastly, we applied the constant false alarm rate based on decision estimation to the Doppler map. Antenna receiver of MSPR goes to the surveillance zone. The receiver antenna reception the straight path signal via side lobes. And it also received other multipath clutter. Particularly, multipath fading is more serious in an urban area, making a good extraction of the reference signals more difficult. Thus, a normal bit error rate (BER) measurement performance will not be enough [27], [28]. Taking into consideration the coherent processing method used for multistatic passive radar processing signals, it is objective to use the correlation coefficient for better access matched transmitted signals. For easy computation, let consider the dynamic notation,

$$r_t = R(r_{t-1}) \quad (1)$$

$R(\cdot)$ represent the dynamic function, this is the stochastic process of the UAV. If we consider the UAV as an agent vulnerable to external environmental and influences, we can come up with this two transitional functions $\mathbb{R} \rightarrow \mathbb{R}$,

$$v_t = V(v_{t-1}, h_1) \quad (2)$$

$$\theta_t = \theta(\theta_{t-1}, h_2) \quad (3)$$

The two stochastics are angular deviation θ_t and UAV speed v_t respectively. As moving in the air, the targets move randomly and independently noises h_1 and h_2 respectively. On the air, this creates a dynamic agent, with description,

$$U_t = I(U_{t-1}, v_t, \theta_t) \quad (4)$$

Where $I(.)$ is the transition function $\mathbb{R}^2 \rightarrow \mathbb{R}^2$, represent the dynamics moves with velocity $U_t = [x'_t, y'_t]^t$, and observation function,

$$o_t = O(U_t, r_t, w_t(n)) \tag{5}$$

o_t represent the observation measurement equation with $O(.): \mathbb{R}^M \rightarrow \mathbb{R}^1$. This define the relationship between two hidden states r_t, u_t and the measurement $o_{t,m}$.

Onward, 3 assumptions have been made here to perform the sensing. Firstly, a periodic assumption, where the drone's emission state is maintained at the same place. Which means r_t will remain constetent for a certain period T_r .

Next, the use of static Gaussian filter. The observation $o_{t,m}$ is relative to the m th radar sensor and the m th moving UAV. Thus, the random noise computation at discrete time t can be written $w_t(n)$ of equation (5), considered to be i.i.d Gaussian noise, with σ_w^2 , also i.i.d.

Lastly, we considered a shifting UAV with a location $U_t = [x'_t, y'_t]^t$ and continue moving with a constant speed at time T_r .

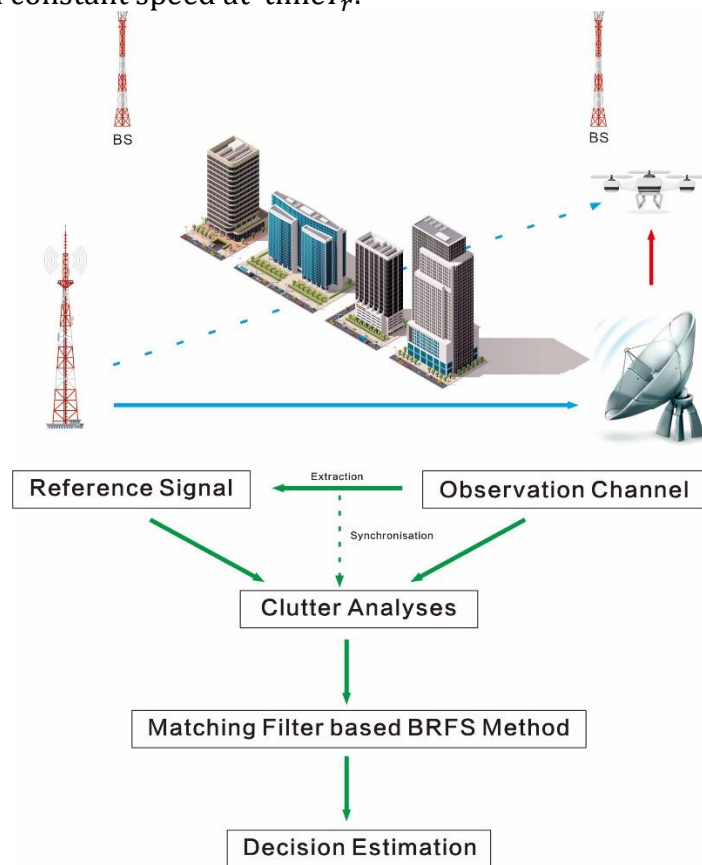


Figure 1. Signal processing flow of a Multistatic Passive Radar.

Its worth to enphazied that those informations are known at the data center. Therefore, the sensing performance, including target localization are

executed at the same time within two main actions. First step, the m th radar sensor will catch the closest target signal at discrete time t , then extract observation data $o_{t,m}$. This is followed by data transportation, which means the radar sensor node will send its observation to the data center for processing. This information are then used in vector's observation $o_t = [o_{t_1}, o_{t_2}, \dots, o_{t_M}]^t$ and target emission state of the positioning can be expressed $r_t(x'_t, y'_t)$.

4.1 Drone's Dynamic Positioning

First of all, UAV statistical movements ,include speed and orientation angle are studied. We have considered that the target is moving in accordance with the random walking process. As two random variables [29, 30], equation (2) and (3), which represent the speed and orientation at time t , can be expressed,

$$v_t = v_{t-1} + h_1 \quad h_1 \sim \mathcal{N}(0, \sigma_v^2) \quad (6)$$

$$\theta_t = \theta_{t-1} + h_2 \quad h_2 \sim \varepsilon(0, \sigma_\theta^2) \quad (7)$$

Where σ_v^2 is the speed variance and σ_θ^2 the direction, with noises $\mathcal{N}(0, \sigma_v^2)$ and $\varepsilon(0, \sigma_\theta^2)$ are i.i.d , subsequently according to random walking process. Following the above inference, according to the speed and orientation, then we have the dynamic Cartesian equations as follow,

$$x_t = x_{t-1} + v_t \cos(\theta_t) \quad (8)$$

$$y_t = y_{t-1} + v_t \sin(\theta_t) \quad (9)$$

Here, UAV cartesian position coordinate are reprsneted by x_t and y_t .

4.2 Statistical Detection

In order to derive a decision rule and the detection analysis, which maximizes $Pr[r_{t+1} = 1 | r_t = 1]$. Based on the observation set $o_{t,m}$, given this realization, the conditional probability of correct detection can be written as,

$Pr[r_{t+1} = 1 | r_t = o_{t,m}]$, Algebraic received signal observation can be written,

$$o_{t,m} = \sum_{n=1}^N [\rho_t \sqrt{E_r} a_t(n) d_{t,m}^{-\alpha/2} + w_t(n)]^2 \quad (10)$$

Where $o_{t,m}$ is signal strength received at m th radar, $d_{t,m}$ represent the length that separates the m th radar sensor and the steering UAV at time t , with a path loss α greater than 2. ρ_t is the received gain at m th radar sensor which is from the sensor's processing devises. $N=Tf$ represent frequency sample size .The UAV process messaging index is represnetd by $a_t(n)$, while $n = 1, 2, \dots, N$. To simplify notation, binary phase shift keying (BPSK) is studied as sampling signal, where $a_t(n) = \{+1, -1\}$, and emission power E_r . In absence of target, in sensing system, signal strength received will just be,

$$o_{t,m} = \sum_{n=1}^N w_t^2(n) \quad (11)$$

When the target is at a moving stage , the observation may also be ambiguous. Therefor, the Euclidean distance between the two elements (radar, sensor, and target) needs to be specified,

$$d_{t,m} \Rightarrow \|U_t - a_m\|_2 = \sqrt{(x'_t - x_m)^2 + (y'_t - y_m)^2} \quad (12)$$

Considering the distance $d_{t,m}$ and emission states r_t , we can write the likelihood density $p(o_{t,m} \setminus d_{t,m}, r_t)$. Considering the fact that N must be very large ($N \geq 100$), by performing the Gaussian densities probability function of i.i.d noise ,we can obtain the likelihood function. Thus, the central limit theorem (CLT) can be estimated by

$$p(o_{t,m} \setminus U_t, r_t) \begin{cases} \prod_{m=1}^M p(o_{t,m} \setminus U_t, r_t = 1) \sim H_1 \\ \prod_{m=1}^M p(o_{t,m} \setminus U_t, r_t = 0) \sim H_0 \end{cases} \quad (13)$$

Therefore, all data can be seen at the data center side, it can also be observed as Gaussian i.i.d ,

$$\begin{aligned} \varphi(o_t \setminus U_t, r_t) &= \sum_{m=1}^M \varphi(o_{t,m} \setminus U_t, r_t) \\ \vartheta(o_t \setminus U_t, r_t) &= \sum_{m=1}^M \vartheta(o_{t,m} \setminus U_t, r_t) \end{aligned}$$

4.3 States Prediction

Bayesian estimations are very sophisticated when comes to unknown function [29, 31], we can estimate the unknown measurement as a random variable. Thus, estimating the posterior probability $P_{t-1}(r_{t-1} \setminus o_{1:t-1})$ at time $t-1$. In the present scenario, the UAV s' trajectory and its emission states are discrete (t th) its described e as $r = \{r_0, r_1, \dots, r_t\}$. Considering the effectiveness of Bayesian approach to study and estimate the hidden variables. The posterior probability and update function of the hidden states r_t can be written as Bayes filter,

$$\begin{aligned} P_{t \setminus t-1}(r_{t-1} \setminus o_{1:t-1}) &= \int p_{t \setminus t-1}(r_{t-1} \setminus r_{1:t-1}) p_{t-1 \setminus t-1}(r_{t-1} \setminus o_{1:t-1}) dr_{t-1} \\ P_{t \setminus t}(r_t \setminus o_{1:t}) &= \frac{p_t(o_t \setminus r_t) p_{t \setminus t-1}(r_t \setminus o_{1:t-1})}{\int p_t(o_t \setminus r_t) p_{t \setminus t-1}(r_t \setminus o_{1:t-1}) dr_t} \end{aligned} \quad (14)$$

Where Equation (14) is the prediction equation, and the two function $P_{t \setminus t-1}(r_{t-1} \setminus o_{1:t-1})$ and $P_{t \setminus t}(r_t \setminus o_{1:t})$ are the transition and likelihood function respectively. Considering the above inference, we can then write a joint distribution density function. Due to UAV constant. Due to the fact that tracking an UAV location can be a very difficult task while in the air, this may lead to a weak sensing or some uncertainties . Thus, from Equation (12) ,the distance must remain dynamic, which can help to identify its actual location at the data center especially when its goes on and off (i.e., H_0 or $r_t = r_0$). In addition, the Bayesian inference likelihood between an UAV and radar sensor with a respective separation length may become unavailable, this will make target

dynamic tracking and localization a little more difficult. The other key point is that without the exact location coordinates of the target, the sensing estimation will be inaccurate. And this may lead to an inaccurate result of the reception, principally for Energy Detection sensing approach.

4.4 Signal Processing based Random Finite State

A Random Finite State (RFS) is an inference of a random variables that can change from one state to another in response to the inputs [32]. The action of UAV being present or not during the sensing period can be treated as another as another random states feature [33-35]. In this work, to deeper understand the dynamic behaviors of the moving target, two hidden states were selected, and this combined random process called random finite state, represented as Φ [36]. Explicitly of a RFS Φ (i.e, number of elements) is a random function that can be estimated following the discrete distribution $\rho(g) = P\{|\Phi| = g\}$, with $g \in \mathbb{N}_0$ and $g = |\Phi|$ is the cardinality of RFS Φ . A RFS Φ is characterized by its cardinality and a group of symmetric joint distribution [32, 37] $\rho(\phi_1, \dots, \phi_g)$, $\phi_1, \dots, \phi_g \in \mathbb{R}^g$. Following the UAV's present stage $|\Phi_t| \in \{0,1\}$, we consider a binary threshold γ_t . This lead to the assumption $\gamma_t = 1$ (i.e., H_1) when the UAV transmit its reference sensing signal at time t , or $\gamma_t = 0$ (i.e., H_0) when there is nothing. Then, we observe that random variable γ_t and the steering distribution $\rho(g)$ are Bernoulli Random Finite States (BRFS). The BRFS can either be zero ($1 - q$) or have one (q). Applying Mahler's theorem [36, 37], the probability density function (PDF) of the finite set statistics (FISST) of this kind of Bernoulli RFS can be written,

$$\rho(g) = \begin{cases} 1 - q & \text{if } \sim \Phi_t = \emptyset \text{ or } \gamma_t = 0 \\ q & \text{if } \sim \Phi_t = \{U_t\} \text{ or } \gamma_t = 1 \end{cases} \quad (15)$$

This can also be written as a random variable based on the the probability density function (PDF) $p(\Phi_t)$ [37],

$$p(\Phi_t = \{\phi_1, \dots, \phi_g\}) = g! \rho(g) p(\phi_1, \dots, \phi_g)$$

By integrating the PDF we have ,

$$\int p(\Phi_t) \delta\Phi = p(\emptyset) + \sum_{t+1}^{\infty} \frac{1}{t!} \int p(\phi_1, \dots, \phi_g) d\phi_1, \dots, d\phi_g \equiv 1 \quad (16)$$

We can noticed that $p(\Phi_t)$ can be integrated to one as it's should be for a probability density function .

Consequently, we can further more say that the actual stage of a moving target during sensing can be identified as $|\Phi_t| = 1$, much more this is similar to the dynamic position U_t . Following our steering distribution $\rho(g)$ and s PDF $p(U_t)$, the FISST can be redefined as

$$\rho(\Phi_t) = \begin{cases} 1 - q & \text{if } \sim \Phi_t = \emptyset \text{ or } \gamma_t = 0 \\ q \cdot p(\zeta) & \text{if } \sim \Phi_t = \{U_t\} \text{ or } \gamma_t = 1 \end{cases} \quad (17)$$

Considering some special cases where, γ_t is greater than 1, then $p(\Phi_t) = 0$.

Therefore, the energy detection of the correlation coefficient to demonstrate how well the reference signal extraction pairing with transmitter signal will be,

$$\rho = \left| \frac{E[S_{Ex}^H S_{Ref}]}{\sqrt{E\|S_{Ex}\|^2} \sqrt{E\|S_{Ref}\|^2}} \right| \quad (18)$$

A set of stationary point scatters can be depicted very well as this is a requirement in the ultrahigh frequency (UHF) band, because its help on modeling the ground clutter and multipath clutter. According to the above expectation, the complex envelope of the total signal in the receiver channel is given by,

$$r_i(t) = H_i^{N^{BS} \times M} x(t) + \sum_j Q_{Mj}^0 H_j^{N^{BS} \times N^{UE}} P_j s_i^{UE}(t) + Q_{Mj}^0 W_j(t) \quad (19)$$

H_i represents interference channel defined as positive finite matrices between the radar and surrounding base station (BS). $x(t)$ represents the complex direct path of the signal, $w_j(t)$ is the white additive Gaussian noise vector with zero mean and covariance Q_{Mj}^0 , P_j are the linear decoding and precoding matrix respectively. The goal of modeling j^{th} precoder and decoder is to identify the null space range with the columns of the decoder matrix ideal to feat signal interferences [38, 39]. Where $i = 1, 2, \dots, k$, and H_i can then be written,

$$H_i = \begin{bmatrix} h_i^{(1,1)} & \dots & h_i^{(1,M)} \\ \vdots & \ddots & \vdots \\ h_i^{(N^{BS},1)} & \dots & h_i^{(N^{BS},M)} \end{bmatrix} (N^{BS} \times M) \quad (20)$$

Here $h_i^{(l,k)}$ represents the carrier coefficient of k^{th} radar, l^{th} mobile base station at i^{th} radar element. H_i are complex Gaussian zero means identical, independent, and distributed, following Rayleigh spreading order. Moreover, feasible and exhaustive interference studies between radar and cellular communication schemes with more than two channels, are developed here [40-42].

To make the extracted reference signal coherent with the transmitted signal and estimate the time delay (TD) which the error estimation can be closer to Cramer-Rao- lower band [43, 44],

$$\sigma \geq \frac{1}{2\pi F_e \sqrt{SNR}} \text{ and } SNR = \frac{2E}{N_0} \quad (21)$$

Where N_0 is the noise power spectral density, F_e is the bandwidth and E is Energy Detection (ED) of the recieved signal defini as,

$$E = \frac{1}{N} \sum_{n=0}^N |y(n)|^2 \quad (22)$$

As the time delay is often made by locating the cross-correlation function,

$$x_n(t) = \sum_{k=1}^N s(t)_{k-1} \cdot r_i(t)_k \quad (23)$$

Where $s(t)_k$ and $r_i(t)_k$ are k^{th} transmitted and received signal sample, respectively, at time instant t . Therefore, the time delay with sampling frequency f_s can be expressed ,

$$TD = \frac{m}{f_s} + \delta \quad (24)$$

$$m = \operatorname{argmax}[x_n(t)]$$

4.5 Antenna Configuration

In this paper, we consider the transmitting antenna to be nonisotropic. Assuming that at the transmitting antenna we have an input power P_t , we consider this to be nonisotropic power density W_t set at certain distance R to the antenna will be,

$$W_t = e_t \frac{P_t}{4\pi R^2} \approx \frac{P_t G_t(\theta_t, \phi_t)}{4\pi R^2} \approx e_t \frac{P_t D_t(\theta_t, \phi_t)}{4\pi R^2} \quad (25)$$

$G_t(\theta_t, \phi_t)$ is the gain and (θ_t, ϕ_t) is the directivity of the transmitting antenna in the direction θ_t, ϕ_t . Since the effective area A_r of the receiving antenna is related to its efficiency e_r and directivity D_r then we have,

$$A_r = e_r D_r(\theta_r, \phi_r) \left(\frac{\lambda^2}{4\pi}\right)$$

The amount of power P_r collected by the receiver can be written according to Equation 25,

$$P_r = e_r D_r(\theta_r, \phi_r) \frac{\lambda^2}{4\pi} W_t$$

And the power ratio between the received to the input shall be,

$$\frac{P_r}{P_t} = e_t e_r \frac{\lambda^2 D_t(\theta_t, \phi_t) D_r(\theta_r, \phi_r)}{(4\pi R)^2} \quad (26)$$

The power received based on Equation 26 considers that the transmitter and receiving antennas are matched to their respective lines of load, this leads to the deduct that the reflection efficiencies are unity, and the polarization of the receiving antenna is polarization-matched to the impinging wave (the polarization loss factor and polarization efficiency are unity). Since our transmitted power is incident upon a target, our radar cross section (σ) of the target which is defined as the area intercepting that amount of power which, when scattered isotropically, produces at the receiver a density which is equal to that scattered by the actual target [45],

$$\delta = \lim_{R \rightarrow \infty} (4\pi R^2 \frac{W_s}{W_i}) \approx \lim_{R \rightarrow \infty} (4\pi R^2 \frac{|E^s|^2}{|E^i|^2}) \approx \lim_{R \rightarrow \infty} (4\pi R^2 \frac{|L^s|^2}{|L^i|^2}) \quad (27)$$

Where δ is the radar cross section or the echo zone in m^2 ; R is the observation length from the UAV in m ; W_i and W_s are incident power density (W/m^2) and scattered power density (W/m^2) respectively. E^i (E^s) is incident (scattered) electric field in V/m ; L^i and L^s are incident and scattered magnetic field respectively in A/m . According to [46], the transmitted power on the target is initially captured and then reradiated isotropically as far as the receiver is at concerned. The amount of captured power P_c is obtained by

multiplying the incident power density of Equation 25 by the radar cross section δ , then we have,

$$P_c = \delta W_i = \delta \frac{P_t G_t(\theta_t, \phi_t)}{4\pi R_1^2} = \delta e_t \frac{P_t D_t(\theta_t, \phi_t)}{4\pi R_1^2}$$

As the power captured by the target is reradiated isotropically, and the scattered power density can be described as

$$W_s = \frac{P_c}{4\pi R_2^2} = \delta e_c dt \frac{P_t D_t(\theta_t, \phi_t)}{(4\pi R_1 R_2)^2}$$

The measurement of the power delivered to the receiver load is given by

$$P_r = A_r W_s$$

The above equation can be represented as the ratio of received power ,

$$\frac{P_r}{P_t} = \delta e_c dt e_c dr \frac{D_t(\theta_t, \phi_t) D_r(\theta_r, \phi_r)}{4\pi} \left(\frac{\lambda}{4\pi R_1 R_2}\right)^2 \quad (28)$$

The input power is expressed by the above equation, and it can consider only the conduction-dielectric losses (radiation efficiency) of the transmitting and receiving antennas. The reflection losses (reflection efficiency) and polarization loss (polarization loss factor or polarization efficiency) are not included .By considering the above lost assumption , we must have ,

$$\frac{P_r}{P_t} = e_c dt e_c dr (1 - |\Omega_t|^2)(1 - |\Omega_r|^2) \delta \frac{D_t(\theta_t, \phi_t) D_r(\theta_r, \phi_r)}{4\pi} \left(\frac{\lambda}{4\pi R_1 R_2}\right)^2 |\widehat{\rho}_w \widehat{\rho}_r|^2 \quad (29)$$

Where $\widehat{\rho}_w$ and $\widehat{\rho}_r$ are vector polarization of the scattered waves and the vector polarization of the receiving antenna respectively. When the polarization is matched with the antennas alignment for maximum directional radiation and reception, the above equation can be reduced as,

$$\frac{P_r}{P_t} = \delta \frac{G_{0t} G_{0r}}{4\pi} \left(\frac{\lambda}{4\pi R_1 R_2}\right)^2 \quad (30)$$

Where $G_{0t} G_{0r}$ are the maximum directivity of the transmission and reception, respectively. The above last three equation analysis represent our radar range equation ,where it relates the power delivered to the receiver load (P_r), to the input power transmitted by the antenna (P_t), after it has been scattered by the target with a radar cross section or echo area δ .

4.6 Agent Dynamic movement

Systematically, according to our actual model the BRFS Φ_t , which is the dynamic transitional function, can also follows Markov process. Therefore equation (14) can be written as,

$$p_{t \setminus t-1}(\Phi_t \setminus \{U_t\}) = \begin{cases} 1 - p(t) & \text{if } \sim \Phi_t = \emptyset \\ p(t) \pi_{t \setminus t-1}(U_t \setminus U_{t-1}) & \text{if } \sim \Phi_t = \{\gamma_t\} \end{cases} \quad (31)$$

And

$$p_{t \setminus t-1}(\Phi_t \setminus \emptyset) = \begin{cases} 1 - p'(t) & \text{if } \sim \Phi_t = \emptyset \\ p'(t) b_{t \setminus t-1} U_t & \text{if } \sim \Phi_t = \{U_t\} \end{cases} \quad (32)$$

Where $b_{t \setminus t-1}$ is the birth and initial density function, which describes the target signal reappearance. Thus, $\pi_{t \setminus t-1}(U_t \setminus U_{t-1})$ means target's dynamic survival transitional density function, according to [47], it can be written as: We pose:

$$v = \left\{ \frac{(\|U_t - U_{t-1}\|_2 - v_{t-1})^2}{2\sigma_v^2} \right\} \text{ and } \mu = \left[-\frac{|\tan^{-1}\left(\frac{y_t - y_{t-1}}{x_t - x_{t-1}}\right) - \theta_{t-1}|}{\sigma_\theta^2} \right]$$

Therefore, the target's dynamic survival transitional density function can be written as,

$$\pi_{t \setminus t-1}(U_t \setminus U_{t-1}) = \frac{1}{\sqrt{2\pi}\sigma_v} \exp(v) \times \frac{1}{2\sigma_\theta} \exp(\mu) \tag{33}$$

$\tan^{-1}(\cdot)$ represent the angular vector, and v_r is UAV's radial speed.

4.7 Filter

This is close to Bayesian prediction, inference, and update process, but here we view the two posterior densities $p_{t \setminus t}(\Phi_t \setminus o_{1:t})$, $f_{t \setminus t}(\Phi_t)$ as a propagation model. That means, in the first step of the prediction the two expression $q_{t \setminus t-1}$ and $f_{t \setminus t-1}(U_t)$ will be derived then we have,

$$\begin{aligned} p_{t \setminus t-1}(\Phi_t \setminus o_{1:t-1}) &= \int P_{t \setminus t-1}(\Phi_t \setminus \Phi_{t-1}) p_{t-1 \setminus t-1}(\Phi_{t-1} \setminus o_{1:t-1}) \delta \Phi_{t-1} \\ &= P_{t \setminus t-1}(\Phi_t \setminus \emptyset) p_{t-1 \setminus t-1}(\emptyset \setminus o_{1:t-1}) \\ &+ \int P_{t \setminus t-1}(\Phi_t \setminus U_{t-1}) p_{t-1 \setminus t-1}(U_{t-1} \setminus o_{1:t-1}) dU_{t-1} \end{aligned} \tag{34}$$

Now we are solving $\Phi_t = \emptyset$ (when the drone is off) with $p_{t \setminus t-1}(\emptyset \setminus o_{1:t-1}) = 1 - q_{t \setminus t-1}$ and $\Phi_t = \{U_t\}$ (when the drone went on) with $p_{t \setminus t-1}(U_t \setminus o_{1:t-1}) = q_{t \setminus t-1} f_{t \setminus t-1}(U_t)$. We can notice that the probability density function FISST is in the form of Equation (26), then we can write:

$$\begin{aligned} q_{t \setminus t-1} &= 1 - [(1 - p_b)(1 - q_{t-1 \setminus t-1}) + (1 - p_s)q_{t-1 \setminus t-1}] \\ &= p_b(1 - q_{t-1 \setminus t-1}) + p_s q_{t-1 \setminus t-1} \end{aligned} \tag{35}$$

Alike, when the UAV goes on, we have the equation,

$$f_{t \setminus t-1}(U_t) = \frac{p_b(1 - q_{t-1 \setminus t-1})b_{t \setminus t-1}(U_t)}{q_{t \setminus t-1}} + \frac{p_s q_{t-1 \setminus t-1} \int \pi_{t-1 \setminus t-1}(U_t \setminus U_{t-1}) f_{t-1 \setminus t-1}(U_{t-1}) dU_{t-1}}{q_{t \setminus t-1}} \tag{36}$$

It is important to mention that the two equations above are the predictable density ($q_{t-1 \setminus t-1}$) and spectral density ($f_{t \setminus t-1}(U_t)$), this may involve two important probability density functions, birth probability of the new appearing target and a survival probability of an existing moving target. The birth probability is described as an appearance of the target during sensing (p_b); and the survival is defined as a continuing presence of the target (p_s) during sensing. The above two assumptions specify the step of Bernoulli filter.

5. EXPERIMENT AND ANALYSIS

This section discusses the output of the experimentation which was mainly generated by Matlab program. Figure 2 depicts the scenario of the drone detection experiment where the passive radar system has a multistatic configuration with one transmitter and four receivers. One of the most important advantages of passive radars is that they are almost undetectable since they do not emit any type of signal. Likewise, they are low-cost and highly portable, making mobile configurations more practical. Thanks to the wide coverage of the transmitter of the signal to be used. Therefore, the transmitter could be any antenna such as a monopole antenna or Guishan tower. Our emitter is a dedicated transmitter, which means the transmitter is intentionally designed and operated to support bistatic signal processing. It's a standard isotropic transmitter that goes up to 360° field of view. The waveform form is set to be user-defined, and this is typical different waveform that can be present during the sensing. In the present case, "1" was chosen as the value to identify a linear frequency modulation waveform. The emitter is mounted to a stationary platform. The origin frequency is 300 mhz and 30Mhz of bandwidth. Our receivers are radar sensors, ideal and isotropic receiver with a 360° field of view. Our sensor is configured as shown in Table 1, with a center frequency of 300 mhz and 30Mhz of bandwidth, and is expected to be LFM waveform so that its can matched the emitter configuration.

The four receivers, marked as Sensors 2, 3, 4, and 5 are set to an inertial navigation system (INS) with an height of about 15m. The measurements between the transmitter and receiver are about 2km -- 3km, accordingly. The antenna receiver pattern is shown in Figure 2. As a cooperative target, we can notice the presence of a quadcopter generating a RF emission, propagation emission, interference losses, and detection. The UAV goes on around the 3D ellipsoid defined by the transmitter and sensor's positioning, and the multistatic measurement. As for now, we know that the target can be anywhere around the ellipsoid, normal single bistatic estimation will not provide the necessity observation of the target. For the localization of the target, using the sense to triangulating its position and achieve the observability of its state, different measurements from multiple sensors are required. That said, the UAV localization algorithm applied in the present work, are principally based on the methodology presented in Equations 27, 28, and 29. If we consider the non-linear nature of the localization signal, this will lead us to two possible target localizations bistatic. Therefore, we can conclude that the target location from two different locations can be possible (or better) when using 3 or more sensors.

In the present experimentation, 4 sensors were considered to achieve the detection goal of the multistatic scheme, we used one emitter, then the target can be seen at a distance (1.5,-0.5,-0.5)Km. Here, the multistatic radar sensors are composed with downward-pointing triangles. The stationary transmitter can be seen in the purple circle shown at the origin. The target is marked with white icon and the grey line demonstrate which trajectory the target is taking.

In 2-D dimension is engraved at Z location of the target as its can be seen b in Figure 3, we can noticed the joined detection in yellow color, located near the intersection zone produced four ellipsoids and is serounding the true position of the target during sensing.

In single-target scenario , we can triangulate the detection to localize the moving object. Consequently, we noticed that in the presence of false alarms and missed detections in multi-target scheme, those informations are not available. This lead into missing data association between the detections sensing and targets. To clear up this issue , we have implemented the statistical detection estimation as discribed in Equation 16,17 and 18. Here, we have estimated the unknown data (read as hidden infomation) associated between the detections and targets and then identify the best solution approach on multi-dimensional chore method. By fusing the detections scheme , we have possible number of the targets and each detection represents a cartesian position of the moving object. As shown in Figure 4, we can noticed a presence of multiple target in 2km of radius and 1Km of distance above ground.

When facing multiple targets and false alarms, the ghost intersections will be more favorable than the traditional solution as shown in Figure 5 (a) , the ghost junctions shown on the scenario, considerably its can be treated as "false alarms" in the data center. We can noticed that the ghost junctions are challenging the true intersections, two true targets are missing at this point. In plot Figure 5 (b), we can noticed a constant tracking,this is maintained on all 5 targets without creating any ghosts or missed detection. Figure 6 (a) and (b) shows the performance historiques of tracks 1 and 2 . This can be seen in orange colors of the tracking. We can also noticed that the tracking histories are near to the true trajectories of the graph. In Figure 6 (c) and (d),Describe the delay between reference signal and observation. This delay is refered as Time delay estimation (TDE).

The Estimation is based on cross-correlation peak position in time.The simulatin we used is the performance of Equation 22 and Equation 24 ,where detected signal was simulated by passing the rectangular pulse through the band pass filter. Rectangular pulse, siumilating the excitation and had a pulsewidth to the half period of the transducer center frequency.Sampling frequency is 100Mhz. The pulse was made by filling the zo's array with the corresponding number of amplitude samples, sognal was shifted by 1 μ s.In case of 5Mhz center frequency and 5% bandwidth the signal is described in Figure 6. (c). Figure 6 (d) discribe ground thruth between technique means and CRLB which is around 1.5%.In Figure 7. Bias errors of -20dBm was compared with CRLB.The TDE was varied within one sample , its can be seen that the experimental result is serounding 0% far away from CRLB. Figure 8 and Figure 9 , we demostrante the reactions of pulse compression, where the transmitted signal pulse undergo modulation until its matched the received signal. In the other side signal-to-noise ratio and the range resolution is improved by the radar systems in using pulse compression and reducing the duration of echoes [48]. Doppler processing is also performed , here the

target's radial velocity is defined by the Doppler shift generated by the target movement.

As shown in Figure 8 , a pulse width of 10 μ s, a pulse iteration frequency of 10 kHz were generated by a linear FM waveform with a stretch bandwidth of 100 kHz. The waveforms generate the matched filter coefficients . To boost Doppler resolution performance , the system emits 64 pulses, and the echoes are stored in Rx signal matrix. The fastest time samples are stored into data matrix stores (time within each pulse) in each column and the slowest time samples (time between pulses) in each row. The results demonstrate that the target is moving at about -50 m/s, and that the target is going away from the transmitter because the speed is negative. The slow time sample plotted in the first place displays the largest peak of about 3000 m, this coincides with the range-speed response pattern plot. The range is determined by the threshold with less than $1e-6$ as the probability of the false alarm. We apply 64 pulses of noncoherent integration in a white Gaussian noise signal. We consider the largest peak above the threshold and perform the estimated target range as seen in Figure 9 (a) the Range Estimation shows 3597.51m. Figure 9 (b) shows the speed estimation of -35.13m/s , Doppler shift is divided by 2, this corresponds to the peak frequency, and it can be transformed into the target speed. When the speed is positive, this means that the target is approaching the transmitter, while when the target is moving away from the transmitter means a negative speed. A briefing parameters and test environment are presented in Table 1.

Table 1. Passive Radar Parameters for Test Environment

Parameter	Values	Parameter	Values
Radar & Drone Communication RF Band	3550-3650 MHz	Update rate	300 MHz
Iterations	2000	Turn Radius	5.5Hz
RCS	$\sigma:0.02m^2$	Radial Velocity	2 Km
Bandwidth	13dB	Doppler spread	100m/s (3×10^8 m/s)
Radar Antenna Tx/Rx	1/4	Spectral efficiency (bits/sec/Hz)	1
Carrier Frequency	300 MHz	Sample Time	0.02
		Gravity - Doppler angular frequency	$9.8 - 4v_r f/c$

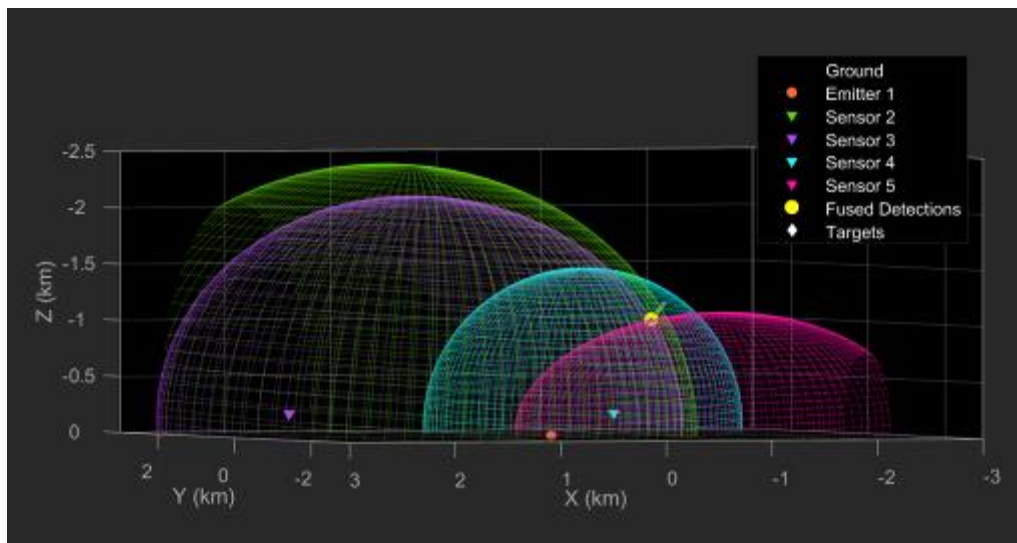


Figure 2. 3D fused spectral target detection position and state estimation.

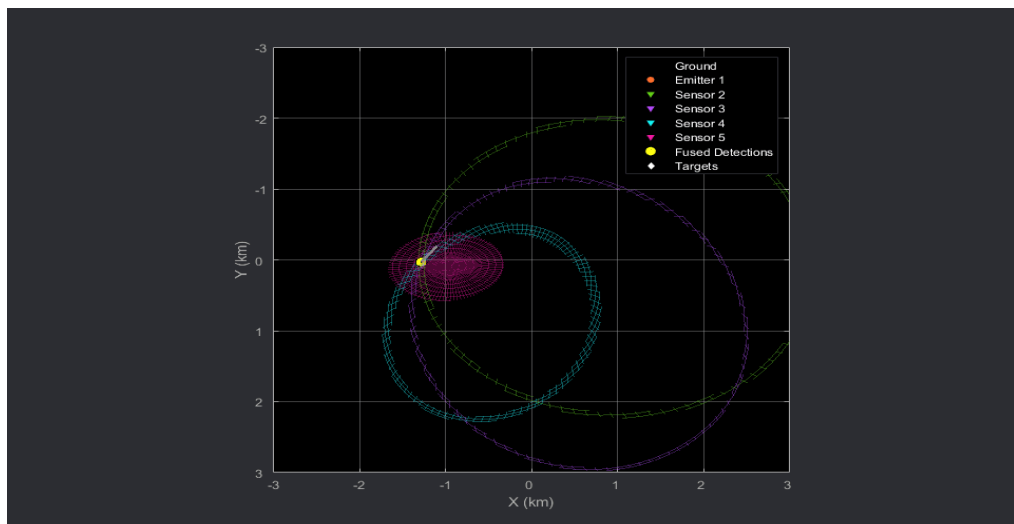


Figure 3. 2D fused spectral target detection surrounding the intersection zone created 4 ellipsoids and its near correct position of the target in sensing time.

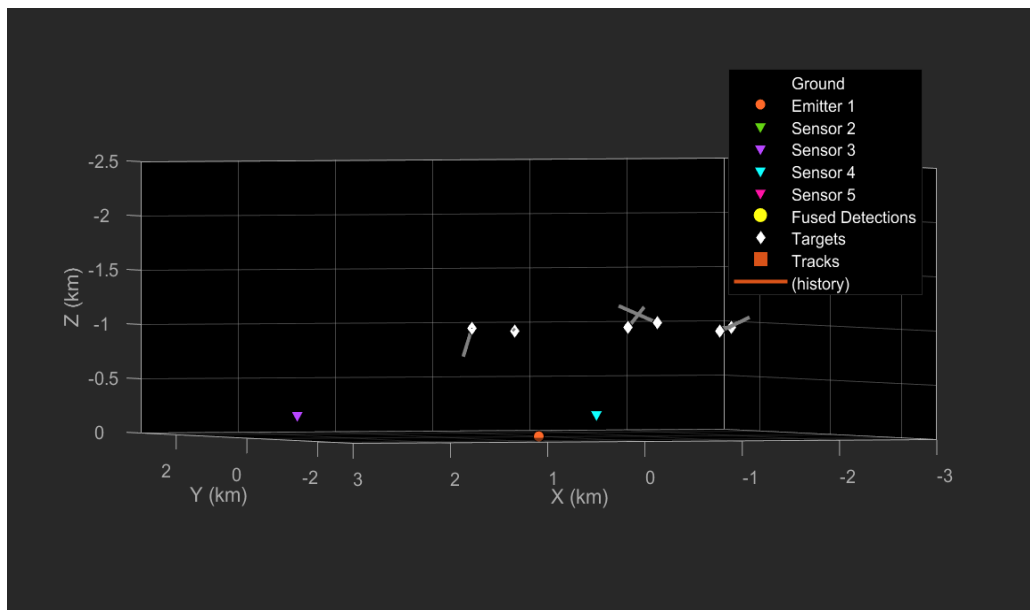


Figure 4. Detection of multi-target and estimation.

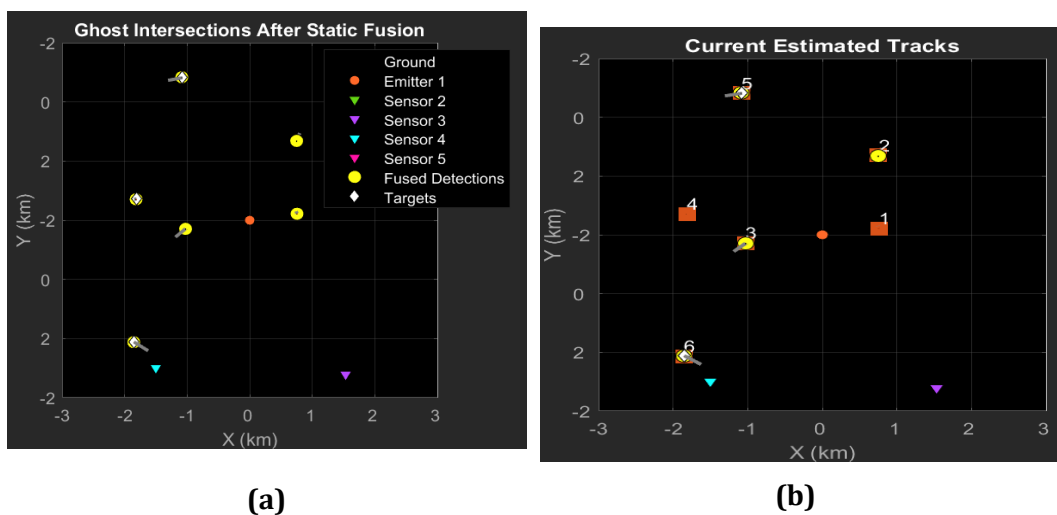


Figure 5. (a) Ghost intersections appearance permormed as "false alarms" through a centralized tracker. As ghost intersections, challenge with the exact intersections.(b) Plot of present trackers estimation.The system is capable of maintaining the tracking on all 5 targets without generating any ghosts or false trackers.

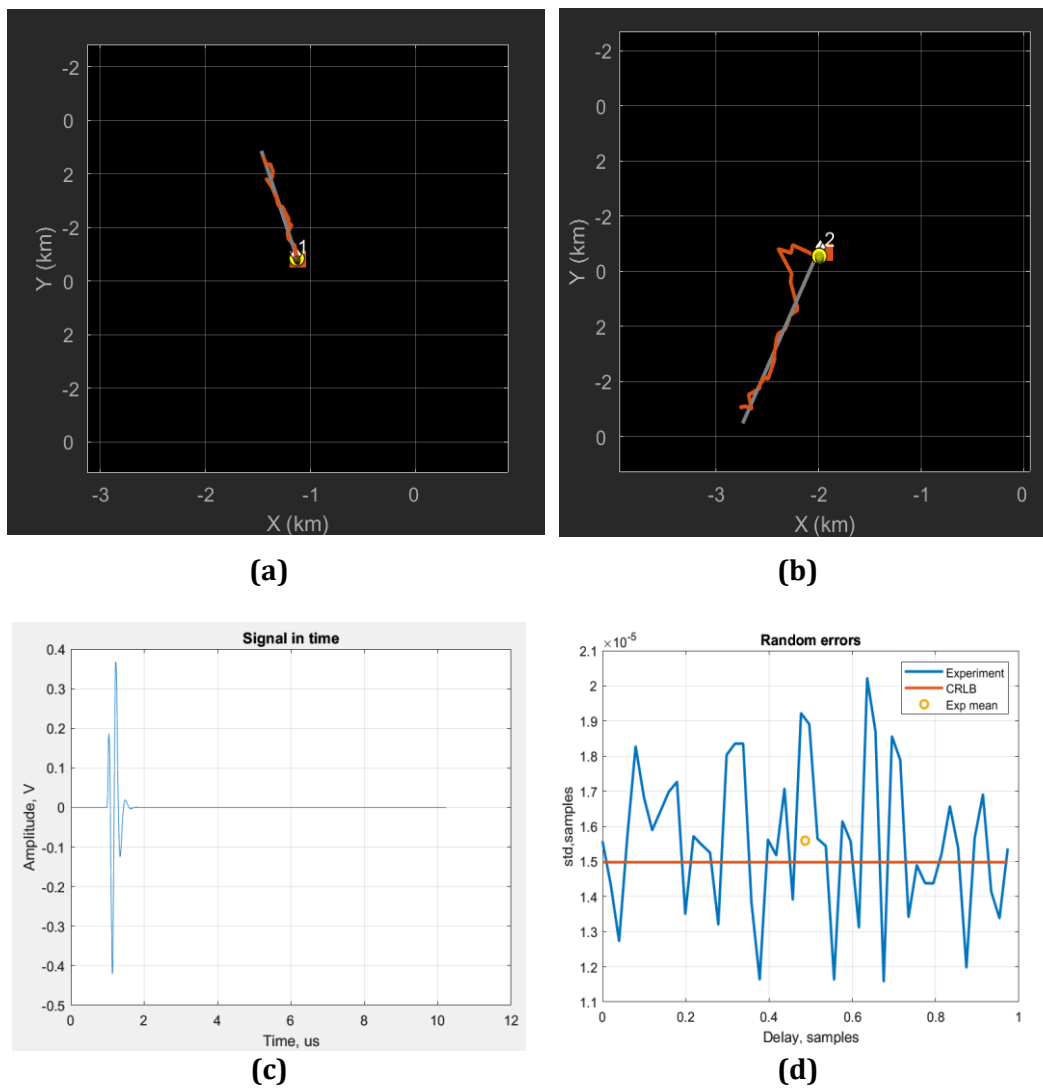


Figure 6. Performance of the top view of tracks (a) and (b), each plot is attached to its history. Each record is displayed by the orange line. And it can be observed that the correct trajectories of the targets are near the tracking histories. (c) Simulation results of 100MHz signal and 50% bandwidth. (d) Ground truth description between technique means and CRLB.

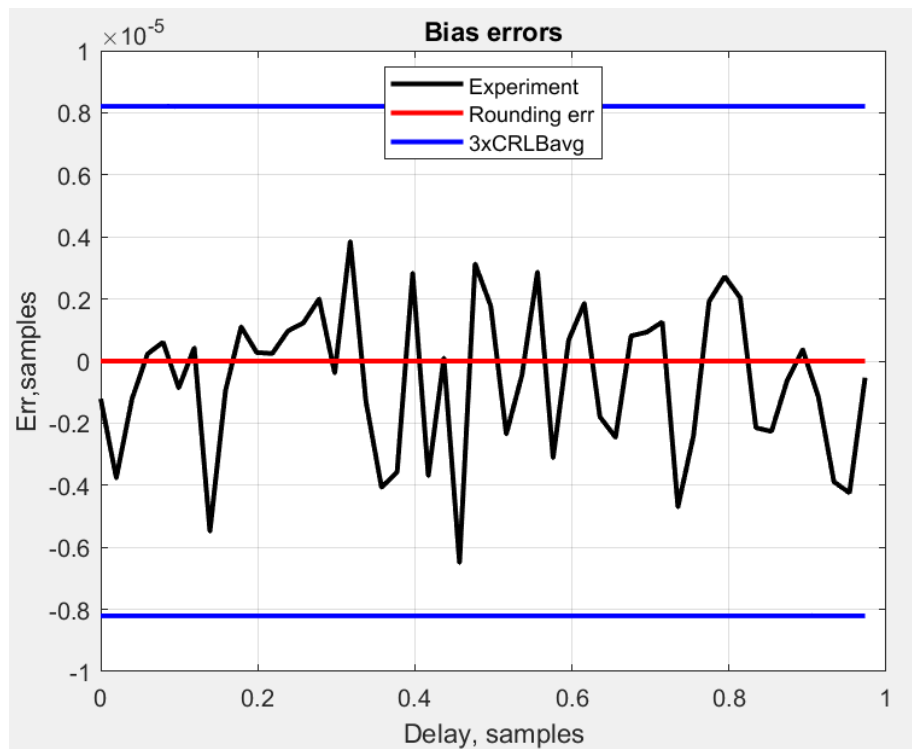


Figure 7. Bias errors of -20dBm compared to CRLB.

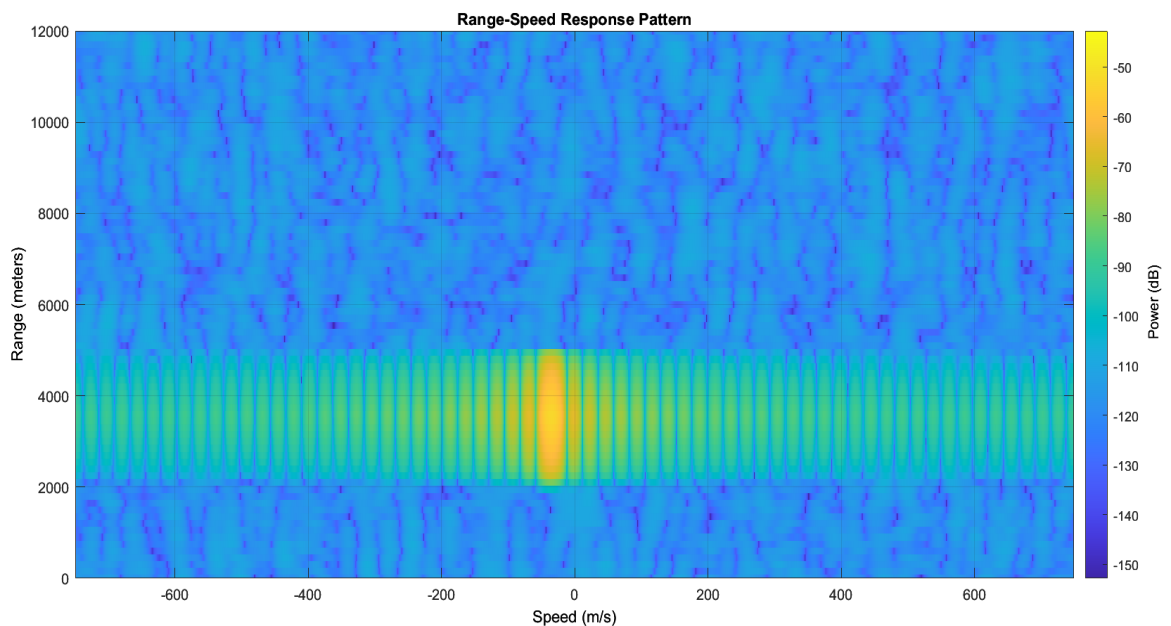


Figure 8. The effects of pulse compression, where the transmitted pulse is modulated and correlated with the received signal. The target is moving at -50 m/s and the largest peak around 3000 m.

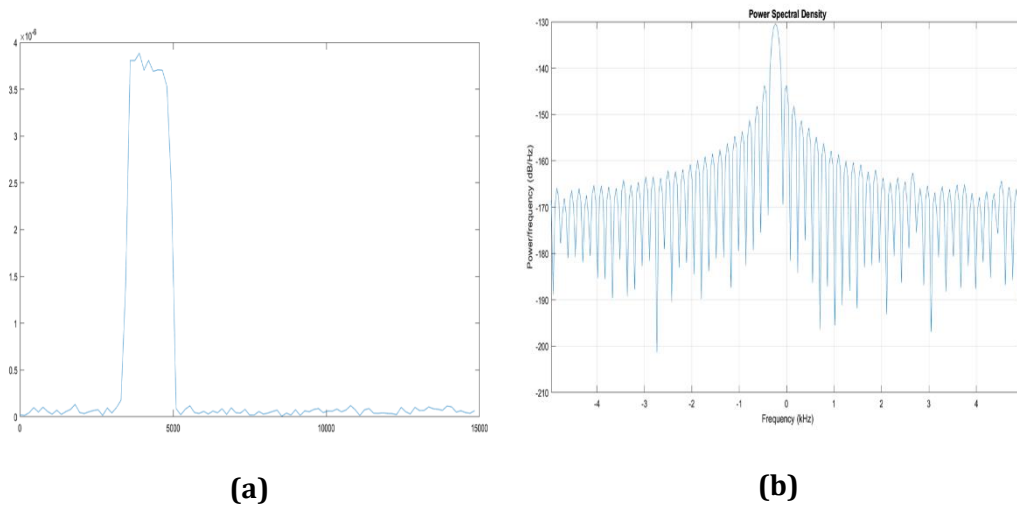


Figure 9. Improvement of Doppler resolution with Range Estimation of 3597.51m. (b) Plot of speed estimation of -35.13m/s ,half of the Doppler shift corresponds to the peak frequency .

5.1 Discussion

The progress of spectrum sensing in cognitive radio network has speeded the use of UAVs and target detection. Consequently, people's privacy and social security have become a great concern. In the present work, we studied spectrum sensing based signal processing for multistatic passive radar for drone detection, and we also considered multitarget detection. In this scenario, we presented a new method concerning the detection, sensing, and tracking of the target. This is followed by a thoughtful signal processing for detection, improvement, and waveform analysis. This is relayed on joint analyses of target localization tracking. We took advantage of the dynamic Bayesian filter approach, more over bernoulli random finite states (BRFS) was applied. What makes this method special is that the hidden emission state of a target can be estimated as a new unknown state, therefore this lead to Markov process for locations indentication. Using the limited data which are available in spectrum sensing, we hinge on the received signal strength to estimate recursively hidden states. Consequently, the approach is very effective in terms of spectrum sharing between the radar system and the moving target airborne localization. The joint distribution is based on Bernoulli Random Finite Set (BRFS) method. Here, the target's emission state and its associated state parameters such as its unknown location are also estimated. Iteratively, we have studied the current location of the target and its next step (prediction), this leads to dynamic positioning analysis, which in most of the times in really live are difficult to estimate. Concerning the antenna configuration, after considering two lossless ($e_{cdt} = e_{cdr} = 1$) X-band (8.2–12.4 GHz) horn antennas were separated by a distance of 100λ . The reflection coefficient at the terminals of the transmitting and receiving antennas were set to 0.1 and 0.2, respectively. The maximum directivities of the transmitting and receiving antennas (isotropic) are 16 dB and 20 dB, respectively. We assuming that the input power of the lossless transmission line connected to

the transmitting antenna is $2W$, antennas are considered aligned at the peak radiation between them and are polarization-matched ($|\widehat{\rho}_w \widehat{\rho}_r|^2=1$) with the help of equation 29, which gives us exactly 4.777 mW as power delivered to the the receiver 's load .By taking full advantage of the OFDM signal's features, we can reconstruct reference signal for digital television broadcasting signal processing, which is essential for the noise and multipath clutter interferences. It also plays an important role especially when the "the reference antenna" drives in the direction of the monitoring zone rather than the transmitter.

When considering mainly 4 procedures: synchronization, channel equalization, soft decoding correction (SDC) or hard decision decoding(HDD),and remodulation, this are the reference signal reconstruction. The closest constellation points are decoded directly by HDD, this does not require much information about the transmitter signal. Except for some cases such as chronization, sampling rate offset calculation, and settlement, it its recommended to select a reasonable method from the SDC and the HDD after the channel equalization to recover the transmitted signal as much as possible.In general, a perfect transmitted reference signal can be obtained through reconstruction via the SDC scheme. Thus, using SDC scheme when SINR of the direct path or the strongest path is very low, it will not be suitable, because the equalized signal will be over the capacity of the decoding and forward error correction.

Moreover, as the direct-path SINR is significantly high, it its not necessary to reconstruct the transmitted signal with the tiring forward error correction, because the transmitted signal can be captured via the simple HDD scheme effectively. To delineate this issue, an experimentation is presented. Principal parameters involved in the simulation are presented in Table 1. It is very difficult to localize and follow the target (tracking) by applying only one passive radar antenna , as a result this can only track the target's bistatic range and bistatic velocity. To face this problem, three distributed single antenna digital-based passive radar stations are needed (minimum) . Together with the signal structure of the digital television broadcasting signal, an multistatic passive radar processing scheme is made possible.This is different to the regular signal processing scheme that each receiving station processes separately information, including reference signal extraction and clutter rejection, this method relayed from the optimal reference signal rebuilt from the receiving station with the least interference as the shared reference signal for all receiving stations.By channel analysis propagation, the receiver station received very less multipath interference, this is taken for optimal signal for the reference signal. Thus, an exact clutter rejection approach is applied to each receiving station. Soon after the detection of CFAR , the data of each Tx-Rx (bistatic) pair are uploaded to the data fusion center. In the data fusion center, data association, elliptical localization technique and matched filter-based Bernoulli random finite states are applied. Following the summary from the algorithm flow, here we have two principal steps:

Use the tracking observation trajectory O_{1t} , and apply Bayesian Filter prediction recursively; apply the update by estimating the posterior density $f_{t|t-1}(U_t)$,

Cleared missing detection with dimension $r_{t-1} = R_0$ as J , and $0 < j < J$, followed by applying the definition of state $r_{t-j-1} = R_1$. Therefore, the drone goes collapsing in stage $\prod_{m=1}^M p(o_{t,m} \setminus U_t, r_t = 0) \sim H_0$ at time $t - J$, and its prediction estimation is subsequently $t - J + m$, (where $m = 1, 2, M$). If the drone continues its move in stage $\prod_{m=1}^M p(o_{t,m} \setminus U_t, r_t = 1) \sim H_1$ at time t , a complete likelihood of the birth density is estimated

$$b_{t \setminus t-1}(X_{t \setminus t-1}) \approx f_v(v_t \setminus \setminus). f_\theta(\theta_t \setminus \setminus) \quad (36)$$

Algorithm Scenario

Iterate

Observation Information Collection,

$$o_{t,m} = \sum_{n=1}^N w_t^2(n), \text{ Equation (11)}$$

Extrat reference signal ρ and Confirm the ration $\frac{P_r}{P_t}$ (Equation (26) and

Equation (30)

Estimation of Dynamic transition RSF Φ_t

$p_{t \setminus t-1}(\Phi_t \setminus \{U_t\})$ Equation (31) and $p_{t \setminus t-1}(\Phi_t \setminus \emptyset)$ Equation (32)

Confirmation of Target survival density: $\pi_{t \setminus t-1}(U_t \setminus U_{t-1})$

Prepare Bernoulli Filters for prediction

$p_{t \setminus t-1}(\Phi_t \setminus o_{1:t-1})$ Equation (34)

For if $i=1$:

 Calculate recursively Bayesian Filter (Prediction)

$q_{t \setminus t-1}$ Equation (35)

 Restore: $f_{t \setminus t-1}(U_t)$ Equation (36)

 Forward Equation (35) and Equation (36) to track

 Clear missed detection with size $r_{t-1} = R_0$,
 where $0 < j < J$ and followt step $r_{t-j-1} = R_1$

End for

Estimate Decision extraction,

$$\prod_{m=1}^M p(o_{t,m} \setminus U_t, r_t = 0) \sim H_0$$

$$i_{min} = \arg \max_{1 \leq i \leq M} \prod_{m=1}^M p(o_{t,m} \setminus U_t, r_t = 0) \sim H_0$$

If not, calculate survival state

$$\prod_{m=1}^M p(o_{t,m} \setminus U_t, r_t = 1) \sim H_1$$

Update the birth density likelihood,

$$b_{t \setminus t-1}(X_{t \setminus t-1}) \approx f_v(v_t \setminus \setminus). f_\theta(\theta_t \setminus \setminus) \text{ Equation (36)}$$

End

Optimum reference signal among multistation can be obtained. It is used as multipath clutter rejection and cross-correlation processing by all stations. System detection performance, adaptability, and robustness can be

improved. As the reference signal is extracted from one of the receiving stations, the other receiving stations have no need to weigh direct-path SINR and target SNR. Multipath clutter cancellation of the multistatic passive radar-based based Bernoulli random finite state (BRFS) is more effective by the optimum extracted signal reference.

It is demonstrated by an extensive numerical experimentation that the system is not only efficient but also potentially accurate in estimating the drone's location and detection. The uncertainty of reception can be measured, therefore, the system can constantly be optimized.

6. Conclusion

As technology are improving, more sophisticated unmanned aerial vehicles are also developed. In this paper, we presented the signal processing scheme, antenna configuration and experimentation performance of the multistatic passive radar based on Bernoulli Finite State for drone tracking and detection. The analysis of the multistatic passive radar detection range has also been reported. According to the peculiarities of digital broadcast signals, pulling of the reference signal was performed and a novel MSPR sensing was suggested. The main goal of this approach is to use the optimal reference signal extracted from the receiving station with the least interference as the shared reference signal, which can greatly improve the system detection capability. Meanwhile, a systematic tracking method for UAV has also been presented. We take full use of Bernoulli random finite state (BRF) estimation for target tracking, localization, and sensing detection of target emission states. Nevertheless, many aspects still need more investigation. MSPR sensing detection, estimation, and multipath fading channel needs to be studied in depth, adding to this various experimentation environments and scenarios. Much more attention will be putted to the very low altitude of moving target, their characteristic classification and identification. Additionally, the MSPR distribution and mobile system optimum network for better detection will also be a point of focus.

Acknowledgments

We will like to thank Zhongshan Institute of Changchun University of Science and Technology for availing materials and resources to contract this research. And the funding support of the Natural Science Foundation of Jilin Province- China under Grant No.201215133, and the Sci-tech Development Project of Jilin Province of China under Grant No. 20130521015JH.

REFERENCES

- [1] Nassi, B., et al. SoK: **Security and privacy in the age of commercial drones**. in *Proc. IEEE Symp. Security Privacy (SP)*. 2021.
- [2] Rizk, Y., et al., **Decision making in multiagent systems: A survey**. *IEEE Trans. on Cognitive And Developmental Systems* **10**(3): p. 514-529.2018
- [3] Chung, T.H., G.A. Hollinger, and V.J.A.r. Isler, **Search and pursuit-evasion in mobile robotics**, *Autonomous Robots*, **31**(4): p. 299-316, 2011.

- [4] Oh, B.-S., et al., **Micro-Doppler mini-UAV classification using empirical-mode decomposition features.** *IEEE Geoscience and Remote Sensing Letters*, **15**(2): p. 227-231, 2017.
- [5] Tahmoush, D. **Detection of small UAV helicopters using micro-Doppler.** in *Radar Sensor Technology XVIII, Int'l Society for Optics and Photonics*, 2014.
- [6] Fioranelli, F., et al., **Classification of loaded/unloaded micro - drones using multistatic radar,** *IET Electronics Letter*, **51**(22): p. 1813-1815, 2015.
- [7] Fuhrmann, L., et al. **Micro-Doppler analysis and classification of UAVs at Ka band.** in **2017, 18th IEEE Int'l Radar Symposium (IRS)**, 2017.
- [8] Rahman, S. and D.A. Robertson. **Millimeter-wave micro-Doppler measurements of small UAVs.** in *Radar Sensor Technology XXI, Int'l Society for Optics and Photonics*, 2017.
- [9] Jahangir, M. and C. Baker. **Characterisation of low observable targets with a multi-beam staring radar.** in *IET Int'l Conf. on Radar Systems (Radar 2017)*. 2017.
- [10] Regev, N., I. Yoffe, and D. Wulich. **Classification of single and multi propelled miniature drones using multilayer perceptron artificial neural network.** in *IET Int'l Conf. on Radar Systems (Radar 2017)*. 2017.
- [11] Björklund, S. **Target detection and classification of small drones by boosting on radar micro-Doppler.** in *2018 15th IEEE European Radar Conf. (EuRAD)*, 2018.
- [12] de Wit, J.M., R. Harmanny, and G. Premel-Cabic. **Micro-Doppler analysis of small UAVs.** in *2012 9th IEEE European Radar Conf.*, 2012.
- [13] Harmanny, R.I., et al., **Radar micro-Doppler mini-UAV classification using spectrograms and cepstrograms,** *Int'l Journal of Microwave and Wireless Technologies* **7**(3-4): p. 469-477, 2015.
- [14] Molchanov, P., et al., **Classification of small UAVs and birds by micro-Doppler signatures.** *Int'l Journal of Microwave and Wireless Technologies*, **6**(3-4): p. 435-444, 2014
- [15] Chen, K., Y. Li, and X. Xu. **Rotating target classification base on micro-Doppler features using a modified adaptive boosting algorithm.** in *2015 Int'l Conf. on Computers, Communications, and Systems (ICCCS)*. 2015. IEEE
- [16] Safaron, M., et al., **Directional cloverleaf antenna for unmanned aerial vehicle (UAV) application,** *Indonesian Journal of Electrical Engineering and Computer Science*, **14**(2): p. 773-779, 2014.
- [17] Liu, Z.-Q., et al., **A novel broad beamwidth conformal antenna on unmanned aerial vehicle.** *IEEE Antennas and Wireless Propagation Letters*, **11**: p. 196-199, 2012.
- [18] Long, K., et al., **Single UWB anchor aided PDR heading and step length correcting indoor localization system,** *IEEE Access*, **9**: p. 11511-11522, 2021.

- [19] Wei, Z., Y.J.I.J.o.A. Junfeng, **A design of vertical polarized conformal antenna and its array based on UAV structure**, *Int'l Journal of Antennas and Propagation*, **11**, p. 1-12, 2017.
- [20] Balderas, L.I., et al., **Low-profile conformal UWB antenna for UAV applications**. *IEEE Access*, **7**: p. 127486-127494, 2019.
- [21] Fang, G., et al., **Experimental research of multistatic passive radar with a single antenna for drone detection**. *IEEE Access*, **6**: p. 33542-33551, 2018.
- [22] Searle, S., S. Howard, and J. Palmer. **Remodulation of DVB—T signals for use in Passive Bistatic Radar**. in *2010 Forty Fourth Asilomar Conf. on Signals, Systems and Computers*. 2010. IEEE
- [23] Kuschel, H., et al. **On the resolution performance of passive radar using DVB-T illuminations**. in *11-th IEEE Int'l Radar Symposium*. 2010.
- [24] Baczyk, M.K., M.J.I.J.o.E. Malanowski, **Reconstruction of the reference signal in DVB-T-based passive radar**. *Int'l Journal of Electronics and Telecommunications*, **57**: p. 43-48, 2011
- [25] Xianrong, W., et al. **Reconstruction of reference signal for DTMB-based passive radar systems**. in *Proceedings of 2011 IEEE CIE Int'l Conf. on Radar*. 2011. IEEE
- [26] Wan, X.-R., et al., **Reference signal extraction methods for CMMB-based passive bistatic radar**. *Journal of Electronics Information Technology*. **34**(2): p. 338-343, 2012
- [27] Balaji, S. and K. Chanthirasekaran. **Per user based Threshold Scheduling to improve Bit Error Rate performance for Multi User MIMO Networks compared to Fair Threshold Scheduling**. in *2022 3rd Int'l Conf. on Intelligent Engineering and Management (ICIEM)*. 2022 .
- [28] Wei, Y., et al., **Research on Information Fusion of Computer Vision and Radar Signals in UAV Target Identification**. *Discrete Dynamics in Nature and Society*, **1**, 2022.
- [29] Miantezila, M., et al. **Primary User Channel State Prediction Based on Channel Allocation and DBHMM**. in *2020 IEEE Int'l Conf. on Cyber-Enabled Distributed Computing and Knowledge Discovery (CyberC)*, 2020.
- [30] Junior, M.M., et al., **Interference Cancellation Based Spectrum Sharing for Massive MIMO Communication Systems**, *Sensors*, **21**(11), p. 3584, 2021.
- [31] Chen, Z.J.S., **Bayesian filtering: From Kalman filters to particle filters, and beyond**. *Hamilton: McMaser University*, **182**(1): p. 1-69, 2003.
- [32] Ristic, B., et al., **A tutorial on Bernoulli filters: theory, implementation and applications**. *IEEE Trans. on Signal Processing*, **61**(13): p. 3406-3430, 2013
- [33] Liang, Y.-C., et al., **Cognitive radio networking and communications: An overview**. *IEEE Trans. on Vehicular Technology*, **60**(7): p. 3386-3407, 2011.

- [34] Lu, L., et al., **Ten years of research in spectrum sensing and sharing in cognitive radio**, *Eurasip J. on Wireless Communications and Networking*, **2012**(1): p. 1-16, 2012.
- [35] Jayaweera, S.K., **Signal processing for cognitive radios**. John Wiley & Sons, 2014.
- [36] Mahler, R.P., **Statistical multisource-multitarget information fusion**. Artech House, Inc, 2007.
- [37] Vo, B.-T. and B.-N. Vo. **A random finite set conjugate prior and application to multi-target tracking**. in *2011 Seventh IEEE Int'l Conf. on Intelligent Sensors, Sensor Networks and Information Processing*. 2011.
- [38] Faragallah, O.S., H.S. El-Sayed, and G.J.I.A. Mohamed, **Performance enhancement of mmWave MIMO systems using deep learning framework**. *IEEE Access*, **9**: p. 92460-92472, 2021.
- [39] Junior, M.M. and B.J.P.o. Guo, **Sensing spectrum sharing based massive MIMO radar for drone tracking and interception**, *PLoS One*, **17**(5): p. e0268834, 2022.
- [40] Antoniadis, N. and A.O.J.I.t.o.s.p. Hero, **Time-delay estimation for filtered Poisson processes using an EM-type algorithm**, *IEEE Trans. on Signal Processing*, **42**(8): p. 2112-2123, 1994.
- [41] Khawar, A., et al. **Beampattern analysis for MIMO radar and telecommunication system coexistence**. in *2014 IEEE Int'l Conf. on computing, networking and communications (ICNC)*. 2014.
- [42] Kim, D.-H., J. Youn, and B.C.J.S. Jung, **Opportunistic Interference Alignment for Spectrum Sharing between Radar and Communication Systems**, *Sensors*, **20**(17): p. 4868, 2020.
- [43] Mahfoudia, O., F. Horlin, and X. Neyt, **On the feasibility of DVB-T based passive radar with a single receiver channel**. *IEEE Int'l Conf. on Radar Systems (Radar 2017)*, 2017
- [44] Schwark, C. and D. Cristallini. **Advanced multipath clutter cancellation in OFDM-based passive radar systems**. in *2016 IEEE Radar Conference (RadarConf)*. 2016.
- [45] Balanis, C.A., **Antenna theory: analysis and design**. John wiley & sons, 2015.
- [46] Stutzman, W.L. and G.A. Thiele, **Antenna theory and design**. John Wiley & Sons, 2012.
- [47] Vo, B.-T., B.-N. Vo, and A.J.I.T.o.s.p. Cantoni, **Bayesian filtering with random finite set observations**. *IEEE Trans. on Signal Processing*, **56**(4): p. 1313-1326, 2008.
- [48] Malanowski, M., K.J.I.t.o.A. Kulpa, and E. Systems, **Two methods for target localization in multistatic passive radar**. *IEEE Trans. on Aerospace and Electronic Systems*, **48**(1): p. 572-580, 2012.